SLAC-PUB-6508
August 1994
(T/E)

Precision Measurement of the Proton Spin Structure Function g_1^{p*}

The E143 Collaboration

K. Abe,[15] T. Akagi,[12,15] P. L. Anthony,[12] R. Antonov,[11] R. G. Arnold,[1] T. Averett,[16] H. R. Band,[17] J. M. Bauer,[7] H. Borel,[5] P. E. Bosted,[1] V. Breton,[3] J. Button-Shafer,[7] J. P. Chen,[16] T. E. Chupp,[8] J. Clendenin,[12] C. Comptour,[3] K. P. Coulter,[8] G. Court,[12,*] D. Crabb,[16] M. Daoudi,[12] D. Day,[16] F. S. Dietrich,[6] J. Dunne,[1] H. Dutz,[12,**] R. Erbacher,[12,13] J. Fellbaum,[1] A. Feltham,[2] H. Fonvieille,[3] E. Frlez,[16] D. Garvey,[9] R. Gearhart,[12] J. Gomez,[4] P. Grenier,[5] K. A. Griffioen,[11,†] S. Hoibraten,[16,§] E. W. Hughes,[12] C. Hyde-Wright,[10] J. R. Johnson,[17] D. Kawall,[13] A. Klein,[10] S. E. Kuhn,[10] M. Kuriki,[15] R. Lindgren,[16] T. J. Liu,[16] R. M. Lombard-Nelsen,[5] J. Marroncle,[5] T. Maruyama,[12] X. K. Maruyama,[9] J. McCarthy,[16] W. Meyer,[12,**] Z.-E. Meziani,[13,14] R. Minehart,[16] J. Mitchell,[4] J. Morgenstern,[5] G. G. Petratos,[12,‡] R. Pitthan,[12] D. Pocanic,[16] C. Prescott,[12] R. Prepost,[17] P. Raines,[11] B. Raue,[10] D. Reyna,[1] A. Rijllart,[12,††] Y. Roblin,[3] L. Rochester,[12] S. E. Rock,[1] O. A. Rondon,[16] I. Sick,[2] L. C. Smith,[16] T. B. Smith,[8] M. Spengos,[1] F. Staley,[5] P. Steiner,[2] S. St.Lorant,[12] L. M. Stuart,[12] F. Suekane,[15] Z. M. Szalata,[1] H. Tang,[12] Y. Terrien,[5] T. Usher,[12] D. Walz,[12] J. L. White,[1] K. Witte,[12] C. Young,[12] B. Youngman,[12] H. Yuta,[15] G. Zapalac,[17] B. Zihlmann,[2] D. Zimmermann[16]

[1] *The American University, Washington, D.C. 20016*

[2] *Institut für Physik der Universität Basel, CH–4056 Basel, Switzerland*

[3] *LPC IN2P3/CNRS, University Blaise Pascal, F–63170 Aubiere Cedex, France*

[4] *CEBAF, Newport News, Virginia 23606*

[5] *DAPNIA-Service de Physique Nucleaire Centre d'Etudes de Saclay, F–91191 Gif/Yvette, France*

[6] *Lawrence Livermore National Laboratory, Livermore, California 94550*

[7] *University of Massachusetts, Amherst, Massachusetts 01003*

[8] *University of Michigan, Ann Arbor, Michigan 48109*

[9] *Naval Postgraduate School, Monterey, California 93943*

Work supported by Department of Energy contract DE–AC03–76SF00515.

[10] *Old Dominion University, Norfolk, Virginia 23529*

[11] *University of Pennsylvania, Philadelphia, Pennsylvania 19104*

[12] *Stanford Linear Accelerator Center, Stanford, California 94309*

[13] *Stanford University, Stanford, California 94305*

[14] *Temple University, Philadelphia, Pennsylvania 19122*

[15] *Tohoku University, Sendai 980, Japan*

[16] *University of Virginia, Charlottesville, Virginia 22901*

[17] *University of Wisconsin, Madison, Wisconsin 53706*

Abstract

We have measured the ratio g_1^p/F_1^p over the range $0.029 < x < 0.8$ and $1.3 < Q^2 < 10$ (GeV/c)^2 using deep-inelastic scattering of polarized electrons from polarized ammonia. An evaluation of the integral $\int_0^1 g_1^p(x,Q^2)dx$ at fixed $Q^2 = 3$ (GeV/c)^2 yields 0.129 ± 0.004(stat.) ± 0.009(syst.), in agreement with previous experiments, but well below the Ellis-Jaffe sum rule prediction of 0.160 ± 0.006. In the quark-parton model, this implies $\Delta q = 0.29 \pm 0.10$.

Typeset using REVTEX

*Work supported in part by Department of Energy contract DE–AC03–76SF00515.

Measurements of the longitudinal and transverse spin-dependent structure functions $g_1(x,Q^2)$ and $g_2(x,Q^2)$ for deep-inelastic lepton-nucleon scattering have become an increasingly important tool in unraveling the complex structures of the proton and neutron. Of particular interest are the integrals $\Gamma_1^p(Q^2) = \int_0^1 g_1^p(x,Q^2)dx$ for the proton and $\Gamma_1^n(Q^2) = \int_0^1 g_1^n(x,Q^2)dx$ for the neutron. Ellis and Jaffe [1] have made sum rule predictions for each integral under the assumptions of SU(3) flavor symmetry and an unpolarized strange sea. Previous measurements of g_1^p [2–5] have found Γ_1^p to be below the Ellis-Jaffe predictions: this has been interpreted to mean that the strange sea and/or the gluons may be significantly polarized, and that the net quark helicity content of the nucleon may be smaller than expected. A fundamental sum rule originally derived from current algebra by Bjorken [6] predicts the difference $\Gamma_1^p(Q^2) - \Gamma_1^n(Q^2)$. Measurements of Γ_1^n from ^{3}He [7] and deuterium [8] targets combined with the most recent proton data [5] are in agreement with this sum rule prediction when QCD corrections [9] are included.

In this Letter we report new measurements of g_1^p at moderate Q^2 that have considerably smaller errors than previous electron scattering experiments in the same Q^2 range (SLAC E80 [2], SLAC E130 [3]) and muon scattering experiments at higher Q^2 (EMC [4] and SMC [5]). The present experiment, E143, used the SLAC polarized electron beam with energies E of 9.7, 16.2, and 29.1 GeV scattering from polarized proton and deuteron targets in End Station A (ESA) to measure g_1^p, g_2^p, g_1^d, and g_2^d. This Letter reports only the g_1^p results at $E = 29.1$ GeV, covering $1.3 < Q^2 < 10$ (GeV/c)^2 and $0.029 < x < 0.8$.

The longitudinally polarized electron beam was produced by photoemission from a strained-lattice GaAs crystal illuminated by a flash-lamp-pumped Ti-sapphire laser operated at 850 nm [10]. Beam pulses were typically 2 μsec long, contained 2–4$\times 10^9$ electrons, and were delivered at a rate of 120 Hz. The helicity was selected randomly on a pulse-to-pulse basis to minimize instrumental asymmetries. The longitudinal beam polarization P_b was measured in ESA using Møller scattering from thin ferromagnetic foils (49% Fe, 49% Co, 2% Va) magnetized by a Helmholtz coil. Results from two detectors (one to detect just one of the final-state electrons, the other to detect both in coincidence) agreed within

errors. The high statistics coincidence measurements had smaller total errors since they were essentially free of background, and were used for the final values of P_b. Corrections were made for electronics dead time, geometric acceptance, radiative losses in the foil, and a small contribution from the atomic motion of the target electrons ($< 1\%$). Tests including reversing the direction of the foil polarization P_f and varying the beam current over a wide range indicated no systematic bias. Values of P_b using six foils of varying thickness agreed to better than 1%. P_b was observed to vary weakly from 0.83 to 0.86 with the continuously monitored photocathode quantum efficiency (QE). An absolute error of $\pm$ 0.02 was assigned to P_b, dominated by the uncertainty in P_f (measured using an induction coil technique) and the observed spread in the daily P_b measurements versus the QE fit.

The beam current was measured for each beam pulse by two independent toroid systems with an uncertainty of $< 1\%$. A steering feedback system kept the average angle and position of the beam at the polarized target essentially constant. Asymmetries induced by changes in beam parameters correlated with helicity were found to be negligible.

The polarized target assembly contained a permeable target cell filled with granules of $^{15}NH_3$ (99.7% isotopic purity) and immersed in a vessel filled with liquid He, maintained at 1 K using a high-power evaporation refrigerator. A superconducting Helmholtz coil provided a uniform field of 4.8 T. The ammonia granules were pre-irradiated [11] with 30 to 350 MeV electron beams to create a dilute assembly of paramagnetic atoms. During the experiment, they were exposed to 138 GHz microwaves to drive the hyperfine transition which aligns the nucleon spins. This technique of dynamic nuclear polarization produced proton polarizations of 65 to 80% in 10 to 20 minutes. The polarization then slowly decreased due to radiation damage: after eight to twelve hours of exposure to the incident electron beam the polarization had dropped to 50 to 55%. Most of the radiation damage was repaired by annealing the target at about 80 K. The electron beam was rastered over the 4.9 cm^2 front surface of the target to uniformly distribute beam heating and radiation damage. After typically ten anneal cycles, the average polarization began to decline and the material was replaced. The target polarization direction was usually reversed after each anneal by adjusting the

microwave frequency. Also, the direction of the magnetic field was reversed several times during the experiment. Approximately equal amounts of data were taken in each of the four polarization/field direction combinations, and the measured asymmetries were consistent for the four data samples. The target polarization P_t was measured using a series LCR resonant circuit and Q-meter detector [12]. The inductance was supplied by an NMR coil embedded in the ammonia granules, calibrated by measuring the thermal-equilibrium (TE) signal near 1.6 K with beam and microwaves off. The total relative systematic error on P_t was 2.5%, dominated by the observed 2.2% rms spread in the TE measurements.

Scattered electrons with energy E' between 6 and 25 GeV were detected in two independent magnetic spectrometers [13] (first used in experiment E142 [7]) positioned at angles of 4.5° and 7° with respect to the incident beam. Electrons were distinguished from a background of pions in each spectrometer using two threshold gas Čerenkov counters and a 24-radiation-length shower-counter array composed of 200 lead-glass blocks. Seven planes of plastic scintillator hodoscopes were used to measure particle momenta and scattering angles.

The experimental asymmetries $A_\parallel$ and $A_\perp$ were determined from

$$A_\parallel \text{ (or } A_\perp) = \left(\frac{N_- N_+}{N_- + N_+}\right) \frac{C_N}{f P_b P_t} + A_{RC}, \tag{1}$$

where the target polarization is parallel (transverse) to the beam direction for $A_\parallel$ ($A_\perp$); N_- and N_+ are the number of scattered electrons per incident charge for negative and positive beam helicity, respectively; C_N is a correction factor for the polarized nitrogen nuclei; f is the dilution factor representing the fraction of measured events originating from polarizable hydrogen within the target; and A_{RC} is the radiative correction.

The dilution factor f varied with x between 0.13 and 0.17; it was determined from the number of measured counts expected from each component of the $^{15}NH_3$ target, which contained about 13% free protons, 65% ^{15}N, 10% ^{4}He, 6% Al, 5% Cu, and 1% Ti by weight. The relative systematic error in f ranged from 2.2 to 2.6%, as determined from uncertainties in the target composition and uncertainties in the expected ratios of cross sections from different nuclei.

The dead-time corrected rates N_- and N_+ were adjusted for contributions from secondary sources (such as e^+/e^- pair production from photons) measured by reversing the spectrometer polarity. These processes showed no measurable asymmetry, and the corrections to the rates were 10% at the lowest x bin, decreasing rapidly at higher x. The factor C_N varied from 0.97 to 0.98, depending on target polarization, and was determined from measured ^{15}N polarizations and a shell-model calculation to determine the contribution of the unpaired p-shell proton.

The internal radiative corrections for both $A_\parallel$ and $A_\perp$ were evaluated using the formulae of Kukhto and Shumeiko [14]. The cross section components of the asymmetry were "externally radiated" according to Tsai [15] to form the "fully radiated" asymmetry corrections A_{RC}. The corrections varied slowly with x and changed $A_\parallel$ by typically $< 2\%$. Systematic errors were estimated based on uncertainties in the $A_\parallel$ and $A_\perp$ models developed to fit all existing data (including the 9.7 and 16.2 GeV data of this experiment) and correspond to relative errors on $A_\parallel$ of typically 2% for $x > 0.1$, increasing to 11% at $x = 0.03$. The statistical errors at low x were increased to account for the removal of elastic tail contributions of up to 25%.

From the measured values of $A_\parallel$ and $A_\perp$ we calculated the ratio g_1^p/F_1^p using the definition: $g_1/F_1 = d^{-1}[A_\parallel + \tan(\theta/2)A_\perp]$, where $d = [(1-\epsilon)(2-y)]/\{y[1+\epsilon R(x,Q^2)]\}$, θ is the electron scattering angle, $y = \nu/E$, $\nu = E-E'$, and $\epsilon^{-1} = 1+2[1+(\nu^2/Q^2)]\tan^2(\theta/2)$. For the ratio of virtual photon total absorption cross sections $R = \sigma_L/\sigma_T$ we used a global fit [16]. The ratio g_1/F_1 is related to the virtual photon longitudinal asymmetry $A_1 = (g_1/F_1) - \gamma^2(g_2/F_1)$, or $A_1 = d^{-1}\{A_\parallel(1+\gamma^2 y/2) - \gamma^2 y A_\perp/[2\tan(\theta/2)]\}$, where $\gamma^2 = Q^2/\nu^2$. The approximation $A_1 = g_1/F_1$ is valid only when $\gamma \approx 0$ or $g_2 \approx 0$.

The values of g_1^p/F_1^p from this experiment at $E = 29.1$ GeV are listed in Table I and are displayed in Fig. 1 along with results of previous experiments. Data from the two spectrometers are consistent in the overlap region $0.07 < x < 0.55$, and therefore have been averaged together. Since the two data sets differ by about a factor of 2 in average Q^2, the comparison indicates no strong Q^2-dependence for g_1^p/F_1^p. The systematic errors include

contributions from P_b, P_t, f, and A_{RC} discussed above, as well as 3 to 5% in d arising from the uncertainty in R.

It can be seen in Fig. 1 that both the previous SLAC data [3] and the higher Q^2 SMC data [5] ($< Q^2 >= 10$ (GeV/c)^2) are in agreement with the data of this experiment, indicating that to a good approximation, g_1/F_1 is independent of Q^2 over the (x, Q^2) range where this ratio has been measured. The SLAC E130 data are plotted assuming $A_\perp = 0$ (the experiment measured $A_\parallel$ only), and the SMC data are plotted assuming $g_1/F_1 \approx A_1$, which is a good approximation at their beam energy of 190 GeV.

Values of xg_1^p at the average $Q^2 = 3$ (GeV/c)^2 of this experiment are shown in Fig. 2. The evaluation at constant Q^2 is model-dependent, and we made the assumption that g_1^p/F_1^p depends only on x [17]. For $F_1^p = (1+\gamma^2)F_2^p/[2x(1+R)]$ we used the NMC fit [18] to F_2^p and the SLAC fit [16] to R. Using the SLAC global fit [19] to F_2^p gives similar results. The systematic errors on g_1^p include an x-dependent error on the ratio F_1^p/d which varies from 2.5% in the mid-x range to 4% at low x and 10% at high x. The integral of g_1^p over the measured range $0.029 < x < 0.8$ is proportional to the area under the data points in Fig. 2, yielding $\int_{0.029}^{0.8} g_1^p(x)dx = 0.120 \pm 0.004 \pm 0.008$, where the first error is statistical, and the second is systematic. We note that the integral is decreased by 0.006 if we assume that both A_1 and A_2 are independent of Q^2 instead of assuming that g_1/F_1 is independent of Q^2.

An extrapolation from $x = 0.8$ to $x = 1$ was done assuming g_1 is proportional to $(1-x)^3$ at high x; this yields $\int_{0.8}^{1} g_1^p(x)dx = 0.001 \pm 0.001$. The extrapolation to $x = 0$ is more model dependent, and could be large if g_1^p were to increase strongly at low x. We studied the x-dependence of g_1^p using our data combined with SMC and EMC data. We observe that, consistent with Regge theory [20], all data for $x < x_{max} = 0.1$ are well-fit (χ^2/d.f.=0.9) by a constant value of $g_1^p = 0.29 \pm 0.02$ at $Q^2 = 3$ (GeV/c)^2 (see curve on Fig. 2). We use this value to estimate $\int_0^{0.029} g_1^p(x)dx = 0.008 \pm 0.001 \pm 0.005$. The systematic error was estimated by varying x_{max} for the fit from 0.03 (for which only SMC and EMC data contribute) to 0.12 (for which the present data dominate). Given the two assumptions that g_1/F_1 depends only on x and that g_1^p is constant at low x, we obtain the total integral

$\Gamma_1^p = 0.129 \pm 0.004 \pm 0.009$. This is in good agreement with the value from SMC [5] asymmetries, $\Gamma_1^p = 0.122 \pm 0.011 \pm 0.011$, obtained at $Q^2 = 3$ (GeV/c)^2 assuming $g_1/F_1 \approx A_1$ is independent of Q^2. Our result is more than two standard deviations below the Ellis-Jaffe sum rule prediction of 0.160 ± 0.006, evaluated using the QCD corrections of Ref. [21] with $\alpha_s = 0.35 \pm 0.05$ at $Q^2 = 3$ (GeV/c)^2 [22].

We can use the quark-parton model and the SU(3) coupling constants $F + D = 1.2573 \pm 0.0028$ and $F/D = 0.575 \pm 0.016$ [23] to extract the total quark contribution to the proton helicity $\Delta q = \Delta u + \Delta d + \Delta s = 0.29 \pm 0.10$, which is small compared to the Ellis-Jaffe prediction $3F - D \approx 0.58$ for $\Delta s = 0$. Using our value of Δq along with the definition $3F - D = \Delta q - 3\Delta s$, we find the strange quark helicity contribution $\Delta s = -0.10 \pm 0.04$, which is negative and inconsistent with zero.

For $Q^2 = 3$ (GeV/c)^2 and for three flavors, the Bjorken sum rule prediction with third order QCD corrections [9] is $\Gamma_1^{p-n} = \Gamma_1^p - \Gamma_1^n = \frac{1}{6}(g_A/g_V)(1 - \alpha_s(Q^2)/\pi - 3.58\alpha_s^2(Q^2)/\pi^2 - 20.22\alpha_s^3(Q^2)/\pi^3) = 0.171 \pm 0.008$, where g_A and g_V are the nucleon axial-vector and vector coupling constants. Note the importance of QCD corrections at the Q^2 of the present experiment. Combining our results for Γ_1^p with the SLAC E142 [7] determination of Γ_1^n we obtain $\Gamma_1^{p-n} = 0.151 \pm 0.014$, which is consistent with the prediction within errors. Combining with SMC deuteron data [8] gives a result that is also in agreement with the prediction, within larger errors. More data, including the deuteron data from this experiment, will be useful in improving the accuracy with which the Bjorken sum rule can be tested, and in learning about the x- and Q^2-dependence of the nucleon spin structure functions.

We wish to acknowledge the SLAC staff for making this experiment successful; H. Wiedemann and the SSRL, and the staffs of the Bates Linear Accelerator, CEBAF, and the Saskatoon Accelerator Laboratory for providing electron beams to pre-irradiate the target material, and N. Shumeiko for help with radiative corrections. This work was supported by Department of Energy contracts: DE–AC05–84ER40150 (CEBAF), W–2705–Eng–48 (LLNL), DE–AC03–765F00515 (SLAC), DE–FG03–88ER40439 (Stanford), DE–FG05–88ER40390 and DEFG05–86ER40261 (Virginia), and DE–AC02–76ER00881 (Wisconsin); by National

Science Foundation Grants 9114958 (American), 9307710 (Massachusetts), 9217979 (Michigan), 9104975 (ODU), and 9118137 (U. Penn.); by the Schweizersche Nationalfonds (Basel); by the Commonwealth of Virginia (Virginia); by the Centre National de la Recherche Scientifique and the Commissariat a l'Energie Atomique (French groups); and by the Japanese Ministry of Education, Science, and Culture (Tohoku).

REFERENCES

* Permanent address: Oliver Lodge Lab, University of Liverpool, Liverpool, U. K.

** Permanent address: University of Bonn, D-53113 Bonn, Germany.

† Present address: College of William and Mary, Williamsburg, Virginia 23187.

§ Permanent address: FFIYM, P.O. Box 25, N-2007 Kjeller, Norway.

‡ Present address: Kent State University, Kent, Ohio 44242.

†† Permanent address: CERN, 1211 Geneva 23, Switzerland.

[1] J. Ellis and R. Jaffe, Phys. Rev. D **9**, 1444 (1974); D **10**, 1669 (1974).

[2] SLAC E80, M. J. Alguard *et al.,* Phys. Rev. Lett. **37**, 1261 (1976); **41**, 70 (1978).

[3] SLAC E130, G. Baum *et al.,* Phys. Rev. Lett. **51**, 1135 (1983).

[4] EMC, J. Ashman *et al.,* Phys. Lett. **B206**, 364 (1988); Nucl. Phys. **B328**, 1 (1989).

[5] SMC, D. Adams *et al.,* Phys. Lett. **B329**, 399 (1994).

[6] J. D. Bjorken, Phys. Rev. **148**, 1467 (1966); Phys. Rev. D **1**, 1376 (1970).

[7] SLAC E142, P. L. Anthony *et al.,* Phys. Rev. Lett. **71**, 959 (1993).

[8] SMC, B. Adeva *et al.,* Phys. Lett. **B302**, 533 (1993).

[9] S. A. Larin and J. A. M. Vermaseren, Phys. Lett. **B259**, 345 (1991) and references therein.

[10] T. Maruyama, E. L. Garwin, R. Prepost, G. H. Zapalac, Phys. Rev. B **46**, 4261 (1992); R. Alley *et al.,* Report No. SLAC–PUB–6489 (1994).

[11] D. G. Crabb *et al.,* Phys. Rev. Lett. **64**, 2627 (1990); W. Meyer *et al.,* Nucl. Instrum. Meth. **215**, 65 (1983).

[12] G. R. Court *et al.,* Nucl. Instrum. Meth. **A324**, 433 (1993).

[13] G. G. Petratos *et al.,* Report No. SLAC–PUB–5678 (1991).

[14] T. V. Kukhto and N. M. Shumeiko, Nucl. Phys. **B219**, 412 (1983); I. V. Akusevich and N. M. Shumeiko, J. Phys. G **20**, 513 (1994).

[15] Y. S. Tsai, Report No. SLAC–PUB–848, 1971; Y. S. Tsai, Rev. Mod. Phys. **46**, 815 (1974).

[16] L. W. Whitlow *et al.,* Phys. Lett. **B250**, 193 (1990).

[17] G. Altarelli, P. Nason, and G. Ridolfi, Phys. Lett. **B320**, 152 (1994).

[18] NMC, P. Amaudruz *et al.,* Phys. Lett. **B295**, 159 (1992).

[19] L. W. Whitlow *et al.,* Phys. Lett. **B282**, 475 (1992).

[20] R. L. Heimann, Nucl. Phys. **B64**, 429 (1973).

[21] S. A. Larin, Report No. CERN–TH.7208/94 (modified), to be published in Phys. Lett. B.

[22] M. Schmelling and R. D. St.Denis, Report No. CERN/PPE93–193; S. Nerison, Report No. CERN–TH.7188/94.

[23] for example F. E. Close and R. G. Roberts, Phys. Lett. **B316**, 165 (1993); J. Ellis and M. Karliner, Phys. Lett. **B313**, 131 (1993).

FIGURES

FIG. 1. Ratios g_1^p/F_1^p from this experiment (E143) as a function of x. The errors are statistical only. Systematic errors are indicated by the lower band. The average Q^2 varies from 1.3 $(\mathrm{GeV/c})^2$ at low x to 10 $(\mathrm{GeV/c})^2$ at high x. Also shown are data from SLAC E130 [3] and SMC [5].

FIG. 2. The structure function g_1^p (scaled by x) from this experiment evaluated at fixed $Q^2 = 3$ $(\mathrm{GeV/c})^2$. The systematic errors are indicated by the lower band. The curve is given by $g_1 = 0.29$, the value used for the low-x extrapolation.

TABLES

TABLE I. Results for g_1^p/F_1^p from the $E = 29.1$ GeV data of this experiment. The indicated values of Q^2 are weighted by the relative errors in g_1/F_1 for each spectrometer in the overlap region $0.07 < x < 0.55$. Also shown are values of g_1^p evolved assuming g_1^p/F_1^p is independent of Q^2 and evaluating F_1^p at fixed $Q^2 = 3$ (GeV/c)^2.

x	$< Q^2 >$ (GeV/c)^2	g_1^p/F_1^p $\pm$ stat. $\pm$ syst.	g_1^p $[Q^2 = 3$ (GeV/c)$^2]$ $\pm$ stat. $\pm$ syst.
0.031	1.27	$0.048 \pm 0.029 \pm 0.008$	$0.223 \pm 0.132 \pm 0.040$
0.035	1.39	$0.075 \pm 0.022 \pm 0.008$	$0.308 \pm 0.092 \pm 0.037$
0.039	1.52	$0.055 \pm 0.021 \pm 0.008$	$0.203 \pm 0.077 \pm 0.034$
0.044	1.65	$0.091 \pm 0.020 \pm 0.008$	$0.295 \pm 0.066 \pm 0.031$
0.049	1.78	$0.127 \pm 0.020 \pm 0.008$	$0.366 \pm 0.058 \pm 0.028$
0.056	1.92	$0.117 \pm 0.020 \pm 0.008$	$0.300 \pm 0.052 \pm 0.024$
0.063	2.07	$0.114 \pm 0.020 \pm 0.009$	$0.258 \pm 0.046 \pm 0.021$
0.071	2.22	$0.122 \pm 0.020 \pm 0.010$	$0.245 \pm 0.041 \pm 0.019$
0.079	2.49	$0.205 \pm 0.020 \pm 0.011$	$0.368 \pm 0.036 \pm 0.017$
0.090	2.79	$0.164 \pm 0.020 \pm 0.012$	$0.263 \pm 0.032 \pm 0.015$
0.101	3.11	$0.199 \pm 0.020 \pm 0.013$	$0.284 \pm 0.029 \pm 0.014$
0.113	3.40	$0.225 \pm 0.021 \pm 0.014$	$0.287 \pm 0.027 \pm 0.014$
0.128	3.71	$0.212 \pm 0.022 \pm 0.014$	$0.242 \pm 0.025 \pm 0.013$
0.144	4.03	$0.260 \pm 0.023 \pm 0.014$	$0.265 \pm 0.023 \pm 0.013$
0.162	4.38	$0.273 \pm 0.024 \pm 0.015$	$0.249 \pm 0.022 \pm 0.012$
0.182	4.73	$0.318 \pm 0.025 \pm 0.016$	$0.258 \pm 0.020 \pm 0.012$
0.205	5.06	$0.336 \pm 0.027 \pm 0.018$	$0.242 \pm 0.019 \pm 0.012$
0.230	5.41	$0.313 \pm 0.029 \pm 0.020$	$0.199 \pm 0.019 \pm 0.012$
0.259	5.73	$0.419 \pm 0.033 \pm 0.023$	$0.233 \pm 0.018 \pm 0.012$
0.292	6.05	$0.363 \pm 0.037 \pm 0.026$	$0.174 \pm 0.018 \pm 0.011$

0.328	6.40	$0.409 \pm 0.043 \pm 0.028$	$0.167 \pm 0.017 \pm 0.010$
0.370	6.72	$0.403 \pm 0.049 \pm 0.030$	$0.137 \pm 0.017 \pm 0.009$
0.416	7.06	$0.679 \pm 0.058 \pm 0.032$	$0.187 \pm 0.017 \pm 0.008$
0.468	7.37	$0.630 \pm 0.071 \pm 0.034$	$0.138 \pm 0.016 \pm 0.007$
0.526	7.64	$0.635 \pm 0.088 \pm 0.036$	$0.109 \pm 0.015 \pm 0.007$
0.592	8.92	$0.722 \pm 0.133 \pm 0.038$	$0.095 \pm 0.018 \pm 0.007$
0.666	9.05	$0.428 \pm 0.192 \pm 0.040$	$0.041 \pm 0.019 \pm 0.007$
0.749	9.18	$0.837 \pm 0.300 \pm 0.043$	$0.052 \pm 0.019 \pm 0.008$

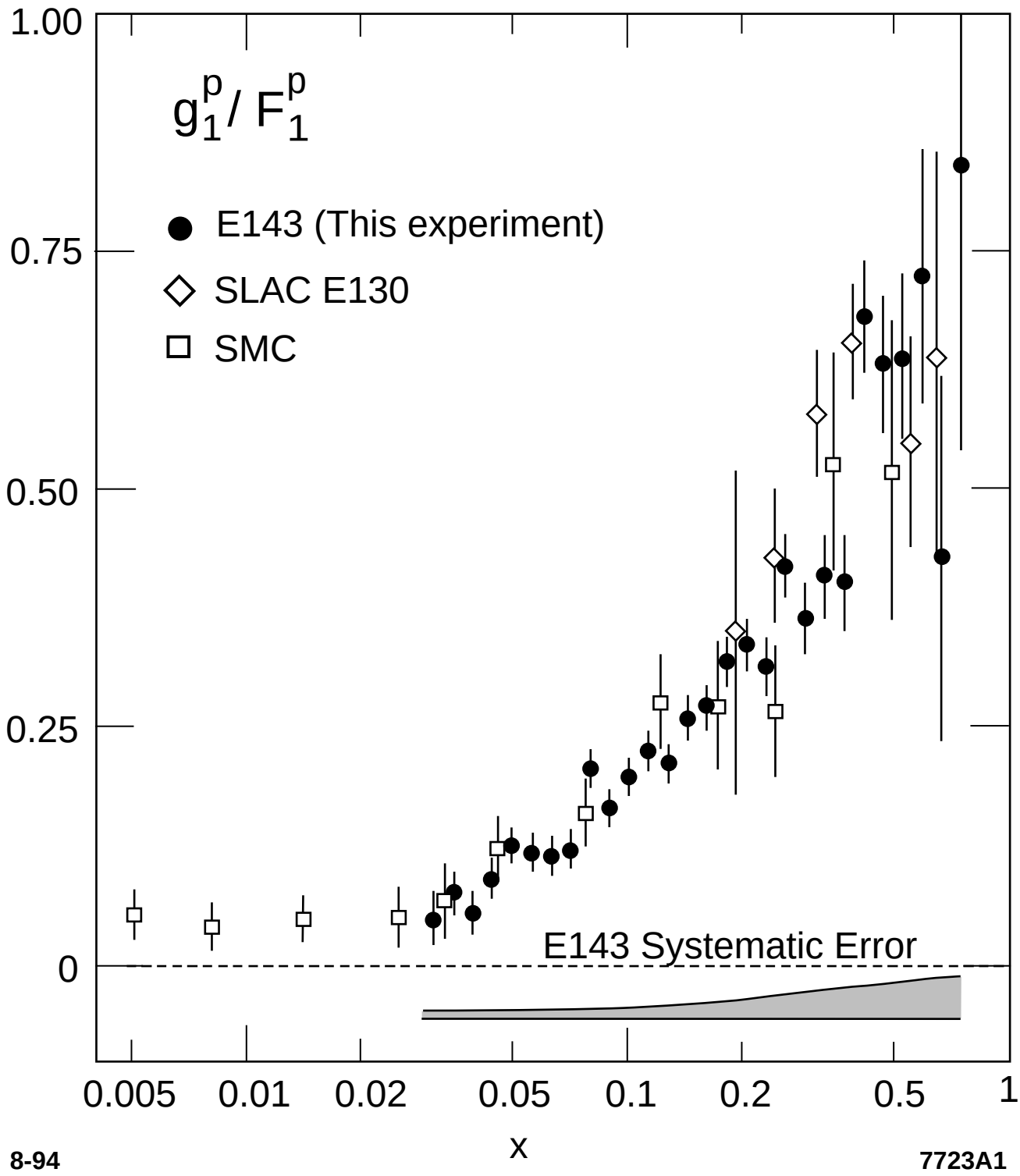
1.00
0.75
0.50
0.25
0
g_1^p / F_1^p
E143 (This experiment)
SLAC E130
SMC
E143 Systematic Error
0.005
0.01
0.02
0.05
0.1
0.2
0.5
1
x
8-94
7723A1

Fig. 1

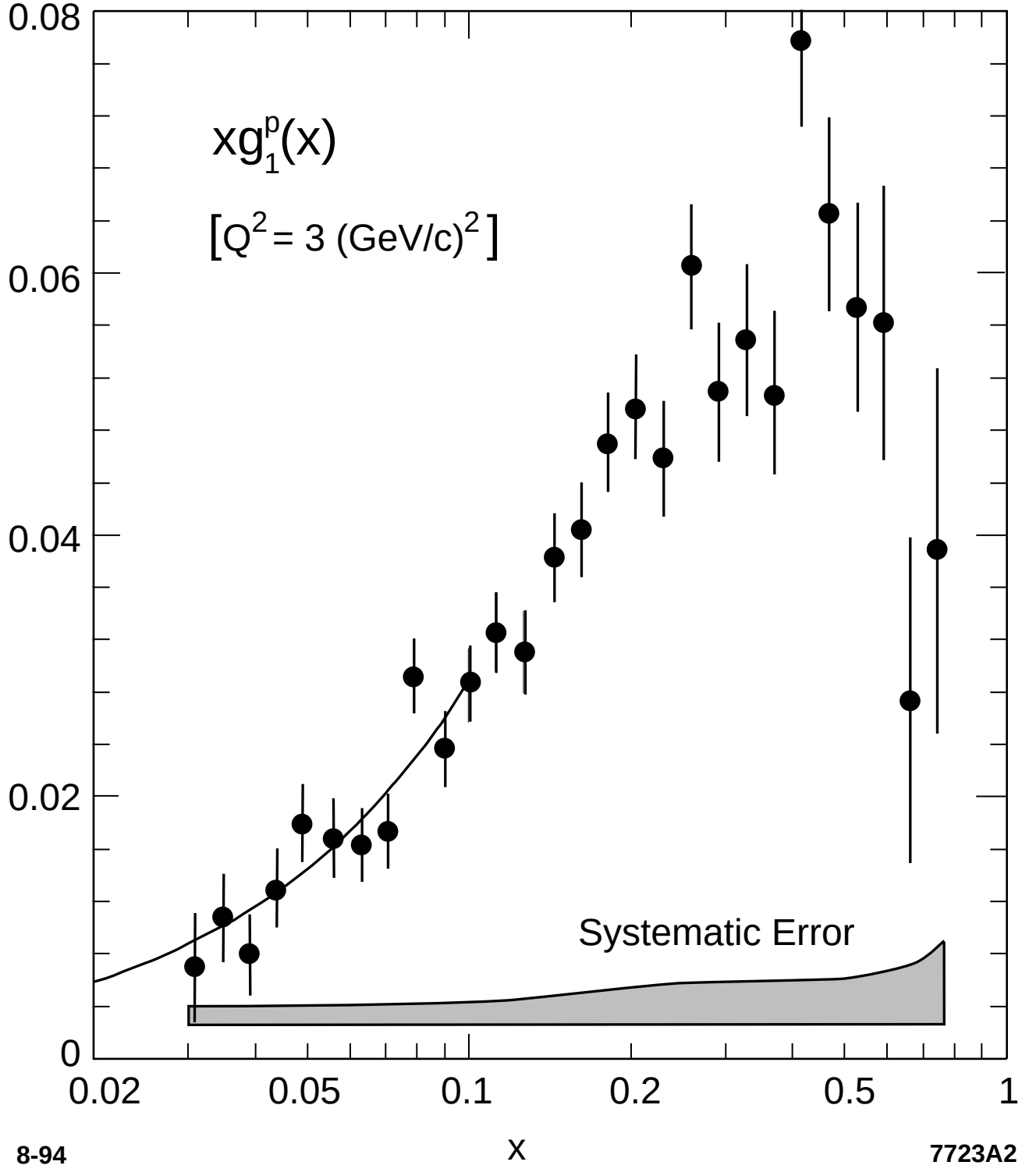
0.08
0.06
0.04
0.02
0
$xg_1^p(x)$
$[Q^2 = 3\ (GeV/c)^2]$
Systematic Error
0.02
0.05
0.1
0.2
0.5
1
x
8-94
7723A2

Fig. 2